

1 Quantifying the impact of gut microbiota on inflammation and 2 hypertensive organ damage 3

4 Ellen G. Avery^{1,2,3,4}†, Hendrik Bartolomaeus^{1,2,3,5}†, Ariana Rauch^{1,2,3,5}, Chia-Yu Chen^{1,2,3,6}, Gabriele
5 N'Diaye^{1,2,6}, Ulrike Löber^{1,2,3}, Theda U. P. Bartolomaeus^{1,2,3,6}, Raphaela Fritsche-Guenther^{2,7}, André F.
6 Rodrigues^{2,3,4}, Alex Yarritu^{1,2,3,5}, Cheng Zhong⁸, Lingyan Fei⁸, Dmitry Tsvetkov^{1,3,6,12}, Mihail Todiras^{2,9}
7 Joon-Keun Park¹⁰, Lajos Markó^{1,2,3,6}, András Maifeld^{1,2,3,6}, Andreas Patzak⁸, Michael Bader^{2,3,6}, Stefan
8 Kempa^{2,11}, Jennifer A. Kirwan^{2,7}, Sofia K. Forslund^{1,2,3,6}, Dominik N. Müller^{1,2,3,6,*}, Nicola Wilck^{1,2,3,5,*}

9 ¹Experimental and Clinical Research Center, a cooperation of Charité-Universitätsmedizin Berlin and
10 Max-Delbrück-Center for Molecular Medicine, Berlin, Germany.

11 ²Max-Delbrück-Center for Molecular Medicine in the Helmholtz Association, Berlin, Germany.

12 ³DZHK (German Centre for Cardiovascular Research), partner site Berlin, Germany.

13 ⁴Department of Biology, Chemistry, and Pharmacy, Freie Universität Berlin, Berlin, Germany.

14 ⁵Charité - Universitätsmedizin Berlin, corporate member of Freie Universität Berlin and Humboldt-
15 Universität zu Berlin, Department of Nephrology and Internal Intensive Care Medicine, Berlin, Germany

16 ⁶Charité-Universitätsmedizin Berlin, corporate member of Freie Universität Berlin and Humboldt-
17 Universität zu Berlin, Berlin, Germany.

18 ⁷Berlin Institute of Health at Charité – Universitätsmedizin Berlin, Metabolomics Platform, Berlin,
19 Germany.

20 ⁸Institute of Translational Physiology, Charité-Universitätsmedizin Berlin, Corporate Member of Freie
21 Universität Berlin and Humboldt-Universität zu Berlin, Charitéplatz 1, 10117 Berlin, Germany.

22 ⁹Nicolae Testemianu State University of Medicine and Pharmacy, Chisinau, Moldova.

23 ¹⁰Hannover Medical School, Hannover, Germany.

24 ¹¹Integrative Proteomics and Metabolomics Platform, Berlin Institute for Medical Systems Biology BIMSB,
25 Berlin, Germany.

26 ¹²Department of Geriatrics, University of Greifswald, University District Hospital Wolgast, Greifswald,
27 Germany

28 † These authors contributed equally.

29 * Address correspondence to: Nicola Wilck, MD Experimental and Clinical Research Center (ECRC)
30 Lindenberger Weg 80, 13125 Berlin, Germany phone: +49-30-450540459 Email: nicola.wilck@charite.de
31 and Dominik N. Müller, PhD Experimental and Clinical Research Center (ECRC) & Max-Delbrück-Center
32 for Molecular Medicine in the Helmholtz Association Lindenberger Weg 80, 13125 Berlin, Germany
33 phone: +49-30-450540286 Email: dominik.mueller@mdc-berlin.de

34 **Keywords:** Hypertension; Microbiome; Inflammation; Kidney; Heart

1 **Abstract**

2
3 **Aims.** Hypertension (HTN) can lead to heart and kidney damage. The gut microbiota has been linked to
4 HTN, although it is difficult to estimate its significance due to the variety of other features known to
5 influence HTN. In the present study, we used germ-free (GF) and colonized (COL) littermate mice to
6 quantify the impact of microbial colonization on organ damage in HTN.

7 **Methods and results.** Four-week-old male GF C57BL/6J littermates were randomized to remain GF or
8 receive microbial colonization. HTN was induced by subcutaneous infusion with angiotensin (Ang) II
9 (1.44mg/kg/d) and 1% NaCl in the drinking water; sham-treated mice served as control. Renal damage
10 was exacerbated in GF mice, whereas cardiac damage was more comparable between COL and GF,
11 suggesting that the kidney is more sensitive to microbial influence. Multivariate analysis revealed a larger
12 effect of HTN in GF mice. Serum metabolomics demonstrated that the colonization status influences
13 circulating metabolites relevant to HTN. Importantly, GF mice were deficient in anti-inflammatory fecal
14 short-chain fatty acids (SCFA). Flow cytometry showed that the microbiome has an impact on the
15 induction of anti-hypertensive myeloid-derived suppressor cells and pro-inflammatory Th17 cells in HTN.
16 In vitro inducibility of Th17 cells was significantly higher for cells isolated from GF than conventionally
17 raised mice.

18 **Conclusions.** Microbial colonization status of mice had potent effects on their phenotypic response to a
19 hypertensive stimulus, and the kidney is a highly microbiota-susceptible target organ in HTN. The
20 magnitude of the pathogenic response in GF mice underscores the role of the microbiome in mediating
21 inflammation in HTN.

22 23 **Translation Perspective**

24 To assess the potential of microbiota-targeted interventions to prevent organ damage in hypertension, an
25 accurate quantification of microbial influence is necessary. We provide evidence that the development of
26 hypertensive organ damage is dependent on colonization status and suggest that a healthy microbiota
27 provides anti-hypertensive immune and metabolic signals to the host. In the absence of normal symbiotic
28 host-microbiome interactions, hypertensive damage to the kidney in particular is exacerbated. We
29 suggest that hypertensive patients experiencing perturbations to the microbiota, which are common in
30 CVD, may be at a greater risk for target-organ damage than those with a healthy microbiome.

31 32 **Introduction**

33 Hypertension (HTN) is the leading risk factor for non-communicable diseases worldwide,¹ and is known
34 as a multifactorial disease, where complex mechanisms often co-occur to lead to a persistent increase in
35 blood pressure (BP). Several studies have indicated that alterations in the composition and function of the
36 intestinal microbiota may contribute to the burden of hypertensive disease.²⁻⁶ However, it is difficult to
37 estimate the contribution of the microbiota, especially in human studies, where the added complexities of

1 other contributing factors easily obstruct our understanding. The aim of our study is to understand the
2 relative contribution that the microbiota has to the burden of hypertensive disease.

3 Mounting evidence suggests that inflammation is not only characteristic of hypertensive cardiovascular
4 disease (CVD) but is causally linked to disease progression and severity.³ Components of both the innate
5 and adaptive immune system have been implicated.³ T helper 17 (Th17) cells and Type 1 helper T cells
6 (Th1) have been shown to be integrally interlinked with hypertensive disease, and have been
7 demonstrated to exacerbate cardiac and renal damage.^{5, 7, 8} Moreover, myeloid derived suppressor cells
8 (MDSC) derived from hypertensive mice were shown to have immunosuppressive properties, and upon
9 adoptive transfer were able to mitigate BP increase in response to angiotensin II (Ang II) infusion.⁹
10 MDSC, Th17, and Th1 cells have each been shown in different settings to be influenced by the
11 microbiota.^{5, 9-11}

12 We and others could recently demonstrate the role of several anti-inflammatory microbial metabolites in
13 HTN. Short-chain fatty acids (SCFA) such as acetate, propionate, and butyrate, are produced by gut
14 microbiota through the fermentation of indigestible dietary fiber.¹² Acetate has been shown to ameliorate
15 hypertensive damage to the kidney and heart in mice.¹³ Our recent work elucidated the protective role of
16 propionate in Ang II-induced inflammation and cardiovascular damage.¹⁴ Furthermore, low butyrate levels
17 have been associated with worsened CVD in several models.¹⁵ In addition to SCFA, we have recently
18 shown that a bacterially produced indole metabolite derived from tryptophan suppresses Th17-driven
19 inflammation in salt-sensitive HTN.⁵ In contrast, metabolites of microbial origin can also exacerbate
20 disease in some contexts. For example, pro-inflammatory metabolites like trimethylamine N-oxide
21 (TMAO) and indoxyl sulfate (IS) have been shown to aggravate CVD.^{16, 17}

22 To address our central aim, we utilized germ-free (GF) mice. C57BL/6J GF littermates were randomized
23 at four-weeks of age to either receive a microbiota transfer from our in-house C57BL/6J colony, or to
24 remain GF for the duration of the experiment. Here we have uncovered several differences between GF
25 and colonized (COL) mice in response to Ang II and 1 % NaCl in the drinking water, which underscores
26 the importance of the microbiota in the pathogenesis of HTN-induced organ damage. Of note, we show
27 an exacerbation of damage in GF mice compared to COL mice, which is more distinct in the kidney than
28 in the heart.

29 **Materials and Methods**

31 *Detailed description of all analytical methods and data analysis used are available in the Supplemental*
32 *Material.*

34 Animal ethics

35 All experiments performed complied with the German/European law for animal protection and were
36 approved by the local ethics committee (G0280/13, G0028/21).

37

1 Animal protocol

2 Wild-type C57BL/6J mice were bred under axenic conditions in an isolator (Metall+Plastic, Radolfzell-
3 Stahringen, Germany). Mice were maintained on a 12:12 hour day: night cycle with constant access to
4 food and water. Until week four, mice in both experimental groups grew up under GF conditions. At four
5 weeks of age male mice were randomized to either remain GF in the isolator or receive passive bacterial
6 colonization (COL). For colonization, mice were introduced in the regular SPF animal facility and placed
7 in cages from healthy wild-type male C57BL/6J mice. Until 12 weeks of age mice received sterilized tap
8 water as drinking water. At 12 weeks of age COL and GF mice received Angiotensin II (Ang II,
9 1.44 mg/kg/d) by subcutaneous infusion via an osmotic minipump (Alzet) and 1% NaCl (Carl Roth) in the
10 drinking water or sham treatment. Sham-treated animals received the same operation procedure without
11 minipump implantation. Minipumps were implanted under sterile conditions, GF mice were kept sterile
12 throughout the experiment. Sterile drinking water was delivered via the Hydropac system (Plexx B.V.,
13 Elst, Netherlands). Throughout the experiment mice were fed autoclaved standard breeding chow
14 (V1124, Ssniff, Soest, Germany). After two weeks of Ang II + 1% NaCl or sham treatment mice were
15 euthanized by isoflurane anesthesia and blood, spot urine (where possible), feces, and organs were
16 collected. The Ang II infusion model was performed in 40 mice (GF n=5, COL n=5, GF+HTN n=16,
17 COL+HTN n=14). Over the course of the experiments five animals were taken out of the experiment
18 (GF+HTN n=3, COL+HTN n=2), due to pre-specified ethical termination criteria in order to counteract
19 severe distress in this experiment. These five mice were not included in the analysis. Additionally,
20 invasive blood pressure measurements were performed in 10 animals (GF n=5, COL n=5), these animals
21 were not included in any other analysis. As a control group for in vitro experiments, cells, and tissues from
22 age-matched conventionally raised SPF C57BL/6J mice (referred to as CONV) were used.

23 Mice were euthanized by isoflurane anesthesia (5% isoflurane-air mixture). Further, echocardiography,
24 blood pressure and Ang II pressor response measurements were performed in isoflurane inhalation
25 anesthesia (2-2.5% isoflurane-air mixture). Details are given in Supplemental Materials.

26
27

28 **Results**

29 ***Absence of microbiota exacerbates cardiorenal damage***

30 To exclude confounding effects relating to the genetic background of mice used in our study, GF
31 littermates were randomized at 4 weeks of age for colonization with SPF microbiota (COL) or further kept
32 under GF conditions. At 12 weeks of age, we induced HTN by subcutaneous Ang II infusion and 1%
33 NaCl-supplemented drinking water. After 14 days, we analyzed hypertensive target organ damage
34 (Figure 1A). Of note, we did not include surgical uninephrectomy to avoid bacterial contamination. The
35 standard model in our lab includes uninephrectomy to induce a more severe form of renal damage^{8, 18},

1 thus we expected a lower degree of renal damage when compared to the published literature.¹⁹ To
2 validate the integrity of our experiment, we first checked the colonization status of the mice. For this,
3 gross morphological changes were assessed, and the characteristics typical of the gastrointestinal (GI)
4 tract in GF mice (e.g., megacecum) did not persist in the mice which had been colonized (COL)
5 (Supplemental Figure S1A). To confirm the microbial status of the respective group, we examined fecal
6 pellets produced on the final day of experimentation. First, pellets were incubated in a thioglycolate
7 medium for 96 hours, and GF mice were found to show no bacterial growth (Supplemental Figure S1B).
8 Second, 16S rDNA copies per gram stool measured by qPCR were found to be similar in COL (Sham and
9 HTN) and conventional SPF mice (CONV), whereas GF mice did not have more 16S rDNA copies than
10 blank samples (Supplemental Figure S1C). Lastly, serum metabolomics confirmed the presence of
11 bacterially derived metabolites in COL mice only (Supplemental Figure S1D). Shotgun metagenomics
12 revealed that the grafted bacteria in COL mice showed the largest overlap with mouse gut metagenomes
13 published in the global microbial gene catalogue (GMGC) (Supplemental Figure S2). We therefore
14 concluded that the GF and COL groups were maintained as intended to confidently proceed with further
15 analyses. Of note, it has been previously reported for the Ang II infusion model that HTN induction leads
16 to changes in the microbiome composition.²⁰ Likewise, we found Ang II infusion influenced the abundance
17 of various taxa in COL mice (Supplemental Figure S1E) as shown by shotgun sequencing. Indeed, both
18 the cecal and fecal compartments displayed differences between the COL sham and HTN groups on
19 phylum and genus levels (Supplemental Figure S1F-G, Supplemental File S1-4).

20 One of the hallmarks of hypertensive target organ damage is renal damage, which is characterized by
21 abnormally high excretion of albumin with the urine (albuminuria), fibrosis, and inflammation. In line with
22 the literature¹⁹, our HTN induction without uninephrectomy led to a moderate increase in albuminuria in
23 COL mice (Figure 1B). GF mice developed a greater degree of albuminuria upon HTN induction, which is
24 abundantly clear when comparing the relative increase of GF and COL mice compared to their respective
25 sham groups (Figure 1B). HTN also led to a significant increase in renal damage marker lipocalin-2 in
26 GF mice (*Lcn2*), which was not evident in COL mice (Figure 1C). Next, we analyzed nephrin, a protein in
27 the podocytes' slit membrane, by immunofluorescence. We observed a significant decrease of nephrin
28 immunofluorescence in GF mice, where COL mice exhibited a similar but insignificant trend (Figure 1D).
29 HTN led to a significant increase of macrophages (F4/80+ cells, Figure 1E) and cytotoxic T cells (CD8+
30 cells, Figure 1F) in the kidney of GF mice, not reaching significance in COL mice. Likewise, we found that
31 mRNA expression of CC-chemokine ligand 2 (*Ccl2*, Supplemental Figure S3A) and infiltrating T cells
32 (CD3+, Supplemental Figure S3B) were selectively increased in the GF group upon HTN. While T helper
33 cells (CD4+ cells) were shown to increase in both GF and COL mice, GF mice displayed a stronger
34 increase (Figure 1G). The number of leukocytes (CD45+ cells) within the kidney confirms the stronger
35 effect of HTN on renal inflammation in GF. (Supplemental Figure S3C). For all immune populations in the
36 kidney, the change in HTN relative to sham was consistently exacerbated in GF compared to COL (Figure
37 1E-G, Supplemental Figure S3B-C). Lastly, we investigated kidney fibrosis. Expression of *Col3a1* was

1 significantly increased only in GF+HTN mice (Supplemental Figure S3D). Perivascular fibrosis analyzed
2 by Masson's trichrome staining was accentuated in GF mice but not statistically different between the
3 groups using two-way ANOVA; although when comparing the relative increase from sham to HTN, there
4 was a significant difference between GF and COL (Supplemental Figure S3E). Similar to what was
5 previously shown²¹, GF mice tended to have lower baseline values for several damage markers when
6 comparing sham-treated GF and COL mice. Overall, renal pathology upon HTN induction was greater in
7 GF mice when compared to their COL littermates.

8 Next, we examined the cardiac phenotype. HTN induction led to greater hypertrophy in GF compared to
9 COL mice, as measured by heart weight-to-tibia length ratio (Figure 2A). Left ventricular weight taken
10 from echocardiography relative to the tibia length (Figure 2B) as well as cardiac *Nppb* expression (Figure
11 2C) confirmed this finding. Neither the GF+HTN nor COL+HTN mice had a reduced ejection fraction
12 (Figure 2D), indicating none of these mice were experiencing systolic heart failure. Using two-way
13 ANOVA, both perivascular (Figure 2E) and interstitial (Figure 2F) fibrosis were significantly increased in
14 GF+HTN and not in COL+HTN mice compared to their respective sham group. Interestingly, when
15 assessing the relative increase in HTN compared to sham for markers of cardiac fibrosis, there was no
16 difference in GF compared to COL mice (Figure 2E-F). Next, we examined cardiac inflammation. Despite
17 an increase in *Ccl2* expression in GF and not COL (Supplemental Figure S4A), macrophages (F4/80+)
18 were increased in both GF and COL hearts upon HTN; and GF+HTN showed significantly less
19 macrophages than COL+HTN mice (Figure 2G). The change in overall leukocytes (CD45+) within the
20 heart mimics the changes seen for macrophages (Supplemental Figure S4B). Furthermore, no
21 significance was reached when comparing CD4+ T helper cell infiltration (Figure 2H), whereas CD8+
22 cytotoxic T cells in the hearts increased in both GF+HTN and COL+HTN mice compared to sham (Figure
23 2I). We also observed an increase in the cardiac expression of pro-inflammatory cytokine *Tnfa* selectively
24 in the GF+HTN group compared to sham (Supplemental Figure S4C). Altogether, cardiac hypertrophy
25 and inflammation following HTN were affected to a greater extent in GF, but when assessing the relative
26 change for GF and COL mice in HTN compared to sham we saw many similarities in the development of
27 the cardiac fibrosis. Whereas in the kidney, there was a clear difference in the development of HTN
28 damage between GF and COL mice, these distinctions were less evident in the heart.

29 ***Hypertensive kidney damage is more sensitive to microbial status than cardiac damage***

30 The aforementioned findings indicate that GF mice respond more sensitively to HTN. Within the context of
31 our initial statistical approach (two-way ANOVA) we often saw a loss of significance for the HTN effect in
32 COL mice under equal statistical power; and the differences between GF and COL response were much
33 clearer when assessing the relative increase for a given marker in HTN (unpaired T-test). To expand on
34 this idea to increase our understanding of the differences between GF and COL, we assessed the size of
35 the HTN-induced effect by calculating an effect size (Cliff's delta) and fold change for each marker. Using
36 a comprehensive univariate testing strategy, we assessed the significance in the different tissue spaces

1 using a robust false discovery rate (FDR) correction within GF and COL groups to root out any spurious
2 findings. From the majority of kidney parameters assessed, across the subcategorizations of damage,
3 fibrosis, and inflammatory markers, a very consistent pattern emerged in that the GF mice experienced
4 worsened kidney outcomes compared to COL mice (Figure 3A, Supplemental Table 1). In contrast to the
5 renal damage, both GF and COL mice experienced a more similar cardiac damage pattern, particularly
6 regarding markers of cardiac fibrosis (Figure 3B, Supplemental Table 2). Albeit several cardiac
7 parameters reached significance in GF and COL mice, the fold changes observed in GF mice were often
8 larger (e.g., *Nppb*, perivascular fibrosis, *Ccn2*, *Lcn2*, F4/80, CD8; Supplemental Table 2). GF+HTN mice
9 develop a significant increase in lung weight-to-tibia length ratio (Figure 3B), indicating the development
10 of lung congestion²² due to aggravated cardiac dysfunction. Taken together, there was more overlap in
11 the cardiac response to HTN in GF and COL groups than was seen for the kidney parameters.

12 To further quantify the HTN effect across the renal (Figure 3C) and cardiac (Figure 3D) tissue space, we
13 performed a multivariate principal coordinate analysis (PCoA) summarizing the overall (dis)similarities
14 amongst the groups. To assess pairwise comparisons of interest, the overall dataset was divided and
15 tested using PERMANOVA (Figure 3C). The pairwise comparisons of the kidney phenotypic data show a
16 significant distance in the COL group from sham to HTN (P-value=0.012, F-value= 4.8). However, the
17 effect of HTN, as measured by the F-value, was greater in the GF mice (P-value= 0.001, F-value= 8.2). In
18 line with our initial univariate targeted analysis (Figure 1), this indicates that the overall phenotypic
19 change in the kidney in response to HTN was larger in GF mice than in COL mice. Furthermore, the
20 pairwise PERMANOVA between GF+HTN and COL+HTN groups (P-value= 0.044, F-value= 3.2)
21 indicates that HTN induction resulted in a different outcome on a multivariate level. Despite some slight
22 differences within some univariate kidney data in the sham groups (e.g., albuminuria, F4/80+ cells),
23 pairwise comparison of GF and COL sham samples was insignificant (P-value= 0.262, F-value= 1.4).

24 For the multivariate analysis of our cardiac data, pairwise comparisons were also used to assess the
25 trajectory of each group (Figure 3D). Consistent with our conclusions from the univariate assessment of
26 the overall cardiac phenotype (Figure 3B), we saw that the comparison between GF+HTN and COL+HTN
27 group showed significant overlap in the PCoA plot, and the pairwise comparison between these samples
28 was not significant (P-value= 0.391, F-value=1.1). Conversely, the difference between sham GF and COL
29 samples was significant, suggesting that perhaps the basal cardiac phenotype is sensitive to the host's
30 microbiome status (P-value = 0.01, F-value = 5.6). As expected, the comparison of HTN to sham samples
31 within the GF (P-value = 0.01, F-value = 4.8) and COL (P-value = 0.046, F-value = 3.2) samples were
32 both significant. The cardiac data again indicate larger phenotypic shifts in GF mice most likely driven by
33 significantly different sham groups.

34 Taken together, our univariate and multivariate approaches indicate a larger effect of HTN in GF mice. In
35 the case of the kidney, this increased effect is indeed driven by a stronger adverse response of GF mice
36 to HTN, whereas in the case of the heart, this effect is driven by phenotypic differences in the healthy
37 groups (sham-treated mice).

1

2 Vascular response to Angiotensin II is similar in GF and COL mice

3 There is some evidence from the literature that vascular reactivity may be dependent on microbial
4 colonization.^{23, 24} We opted not to implant telemetry devices for the measurement of BP in our primary
5 experimental animals, as microscopic vascular surgery was not possible under sterile conditions.
6 Although we decided to forgo this gold-standard for BP measurement, we still questioned whether the
7 axenic status of our GF mice would impact the basal mean arterial pressure (MAP), or BP reactivity to
8 Ang II. We therefore colonized additional mice using the same colonization procedure as previously
9 outlined, and we performed *in vivo* BP measurements using an implanted arterial catheter in freely
10 moving mice. Interestingly, we found that GF mice had a significantly higher MAP (Figure 4A) than their
11 colonized counterparts, although the mean of each group (GF mean value = 118.4 mmHg, COL mean
12 value = 107.8 mmHg) was still in a range considered normal for untreated C57BL/6J mice.²⁵ Acute
13 intravenous infusion of Ang II induced an increase in BP (Figure 4B) which was nearly identical for GF
14 and COL mice, suggesting that AngII-dependent reactivity of the vasculature is similar in these mice.
15 Similarly, we investigated *ex vivo* vascular contractility of mesenteric arteries isolated from conventionally
16 colonized mice (CONV) or GF mice (GF). CONV mice were used for this *in vitro* experiment due to ease
17 of availability because colonization of GF mice is a lengthy procedure. GF mice showed similar contractile
18 response compared to CONV mice in response to Ang II (Supplemental Figure S5A). Additionally,
19 mesenteric arterial rings from GF mice showed similar contraction force in response to KCl to CONV mice
20 (Supplemental Figure S5B). Similarly, endothelial-dependent (Supplemental Figure S5C) and –
21 independent (Supplemental Figure S5D) relaxation was not influenced by colonization status.

22

23 Microbiota and microbial metabolites shape serum metabolome changes in hypertension

24 Although the vascular reactivity of GF mice was similar to those housing microbes, we were interested to
25 understand the different phenotypic and inflammatory response to HTN. We therefore decided to
26 investigate the microbiome itself and associated metabolite production, as our group and others have
27 previously shown that some metabolites of microbial origin can be anti-inflammatory in hypertension.^{5, 13,}
28 ¹⁴

29

29 Consistent with the literature²⁰, the metabolome of GF and COL animals was affected by HTN induction.
30 We found a multitude of differences when analyzing the serum metabolome (MxP Quant 500, Biocrates)
31 from GF and COL mice in HTN compared to the respective sham, which we grouped together by class to
32 show the composite shift of over 300 individually measured metabolites (Figure 5A, Supplemental Table
33 3). Of the 15 classes of metabolites where HTN induction had an effect, four of those classes
34 (phosphatidylcholines, hexosylceramides, alkaloids, fatty acids) showed similar trajectories, suggesting
35 these classes changed in a microbiome-independent manner upon HTN (Figure 5A, individual
36 metabolites shown in Supplemental Figure 6A-D). For individual metabolites, we compared the impact of
37 HTN induction on metabolite trajectories. When comparing sham to HTN, there was little overlap between

1 the metabolites that decreased (Figure 5B) or increased (Figure 5C) within GF or COL. Overall, in GF
2 mice more metabolites were regulated by HTN than in COL mice (Supplemental Table 11) (Figure 5D). Of
3 note, a subset of metabolites which were upregulated in GF mice were downregulated in COL mice in
4 response to HTN and vice versa (Figure 5D, shown in black). Taken together, the alterations of the
5 metabolome in response to HTN show little overlap in GF and COL mice (Figure 5D, shown in purple).
6 Unsurprisingly, the serum metabolome was significantly impacted by the microbiome, and we saw a wide
7 range of correlations between individual metabolites and microbial species, as well as functional modules
8 derived from shotgun sequencing data (Supplemental Figure S7). Although the serum metabolite
9 measurements used here were very comprehensive, they did not cover SCFA metabolites, which we and
10 others have shown to have high importance in the progression of HTN. It has been demonstrated
11 elsewhere that GF mice are devoid of some important SCFA²⁶. We confirmed this for our mouse colonies
12 (GF and CONV, which were the source populations for our experiments) by performing mass
13 spectrometry measurements of fecal acetate, propionate, and butyrate (Fig 5E). We expect that the lack
14 of the potent anti-hypertensive metabolites propionate and butyrate influences the phenotype seen in GF
15 mice.

16

17 ***Inflammation contributes to the differing phenotypic response to HTN in GF and COL mice***

18 It has been shown that the immune system and the gut microbiome are strongly interconnected, and
19 several studies have shown the importance of immune cells in HTN.^{2, 3} We and others have also shown
20 that metabolites of microbial origin can influence inflammation in HTN.^{5, 13, 14} We examined the splenic
21 immune cell composition a surrogate for systemic inflammation in GF and COL mice by flow cytometry
22 (gating strategies are shown in Supplemental Figure S8). Of the 23 immune cell subsets we investigated,
23 12 were differentially influenced by HTN when compared to the respective sham group (Fig 6A,
24 Supplemental Table 4). We then examined all immune parameters multivariately to assess how changes
25 in immune cells would be reflected in the distance between each group using PCoA (Figure 6B). It is
26 known that the immune system of GF mice differs from their colonized counterparts²⁷. Our data confirms
27 this observation as the pairwise comparison of sham-treated GF and COL mice (P-value = 0.011, F-
28 value = 6.6) was significant. Interestingly, this difference between COL and GF was still evident after HTN
29 induction (P-value = 0.026, F-value = 2.8). Pairwise comparisons of individual groups using
30 PERMANOVA indicated that the HTN to sham comparison was significant in the GF group (P-value =
31 0.006, F-value = 4.8), but not within the COL group (P-value = 0.177, F-value = 1.6) (Figure 6B). It can be
32 concluded that overall, the inflammatory status of GF mice was disturbed to a greater degree by HTN
33 induction.

34 Previous studies have shown that splenic MDSC increase in HTN and have anti-hypertensive properties.⁹
35 In line with the literature, there was an increase in monocytic MDSC (mMDSC) upon HTN induction, and
36 this increase was only significant in COL+HTN mice (Figure 6C). Furthermore, for both mMDSC and
37 granulocytic MDSC (gMDSC) (Figure 6D) subtypes, COL+HTN mice showed a significantly higher

1 frequency of these anti-hypertensive immune cells than GF+HTN mice. The relative increase in HTN
2 compared to sham for mMDSC was lesser in GF mice but greater for gMDSC than in COL (Figure 6C-D).
3 The dynamics of whether the relative increase, or absolute number of MDSCs is relevant in HTN is
4 currently unknown. Additionally, we saw an increase in Th17 cells in both GF and COL mice, though this
5 effect only reached significance in GF mice (Figure 6E). This increase was driven by pathological Th1-like
6 Th17 cells, defined by their co-expression of ROR γ t and Tbet (Figure 6F).²⁸ Recent evidence suggest
7 that pre-existing conditions can influence naïve T cell responses towards effector differentiation.²⁹⁻³¹ We
8 hypothesized that the absence of microbes and their metabolites in GF mice would render naïve T cells
9 more vulnerable to cytokines. Therefore, we performed an *in vitro* Th17 polarization of naïve T cells from
10 GF and CONV mice (which were used in place of COL due to ease of accessibility) in the presence or
11 absence of Ang II. Naïve T cells from GF mice more readily polarized towards Th17 cells than cells from
12 CONV mice, particularly in the presence of Ang II (Figure 6G). To demonstrate that the conditions for the
13 polarization of Th17 cells indeed exist *in vivo*, we quantified the expression of each of the Th17-polarizing
14 cytokines (Il-6, Il-1b, and TGF β) by qPCR from kidney (Supplemental Figure S9A, Figure 3A) and heart
15 (Supplemental Figure S9B, Figure 3C) tissue. These key cytokines were increased upon HTN. The
16 comparison of effect sizes (Figure 3A, C) often indicated larger effects of HTN in GF mice. We suspected
17 that the reason naïve CD4+ T cells isolated from CONV mice were less inducible toward Th17 in the
18 presence of Ang II may be due to the priming of immune cells by SCFA in the *in vivo* microenvironment.
19 To test this hypothesis, prior to Th17 induction in the presence of Ang II, naïve CD4+ cells were pre-
20 treated for 24 hrs with the SCFA butyrate and propionate. While the pre-treatment did not affect the
21 induction of Th17 in CONV, SCFA pre-treatment prevented the enhanced Th17 induction of naïve T cells
22 from GF mice (Figure 6H).

23
24 In summary, our *in vitro* findings suggest that the different pre-conditioning of naïve T cells within GF and
25 COL mice may impact polarization into pro-inflammatory effector T cells and thus severity of target organ
26 damage. We anticipate that this effect contributes to our *in vivo* findings, where the absence of microbes
27 and microbiota-derived metabolites like SCFA had a potent impact on immune cells relevant in HTN and
28 cardiorenal damage.

29 30 Discussion

31 Gut microbial dysbiosis associates with HTN in humans^{5, 32} and in rodent models.^{5, 32-34} Fecal microbiota
32 transplantation from hypertensive patients into mice has also been shown to induce an increase in blood
33 pressure.³² However, few studies have focused on the overall contribution of the microbiome to the
34 pathogenesis of HTN, such that it may be contextualized relative to other known contributors to
35 hypertensive disease burden. Here we show in a presence/absence scenario, that the microbiota has a
36 potent effect on HTN-induced cardiac and renal damage in mice. GF mice showed a stronger adverse
37 response to HTN than their COL littermates. Interestingly, the kidney seems to be more sensitive to

1 changes in microbial status than the heart. Lastly, we propose that the altered inflammatory response in
2 GF mice contributes to their aggravated phenotype in HTN.

3 We have shown robustly that the kidney damage within GF mice upon HTN is comparatively more severe
4 than the damage experienced by their COL littermates. Some of the larger effects in our univariate
5 analysis may be related to the slightly lower baseline level of putative markers for kidney damage within
6 sham GF mice compared to sham COL, though these groups do not significantly differ. We surmise that
7 the baseline differences between GF and COL mice are likely due to the immunological uniqueness of GF
8 mice, which has been documented in the literature.²⁷ Indeed, across renal damage, fibrosis and
9 inflammation markers, we consistently saw a significant effect of HTN selectively in the GF group (Fig
10 3A). Furthermore, we show on a multivariate level that the difference between sham GF and GF+HTN
11 mice for the composite of kidney parameters is significant, while the equivalent comparison within the
12 COL mice is insignificant (Figure 3C). Consistent with other inflammatory markers, we show an increase
13 of infiltrating macrophages (F4/80+ cells, Figure 1E) in GF+HTN kidneys, as well as the increased
14 expression of *Ccl2* (Supplemental Figure S3A), which has been implicated as a major player in worsening
15 kidney damage in mice³⁵ and humans³⁶. Infiltrating macrophages during renal injury are known to
16 contribute to the secretion of cytokines like IL-1 β , which enhances the activation and differentiation of
17 Th17 cells.³⁷ A previous study additionally showed that SCFA-treatment in ischemia-reperfusion injury
18 (IRI) radically reduced kidney *Ccl2*, *Il-1b*, and associated kidney damage.³⁸ SCFA have been shown to
19 have anti-inflammatory properties in several cell types³⁹⁻⁴², which could contribute to the lessened
20 damage in COL mice, since only mice harboring microbiota have significant SCFA production within the
21 gastrointestinal tract (Figure 5C). Our results are highly compatible with previous studies showing that GF
22 status exacerbates kidney damage in the context of IRI⁴³ and adenine-induced chronic kidney disease^{21,}
23 ⁴⁴.

24 Intriguingly, we found that the cardiac phenotype was less influenced by the microbial status of the host.
25 Here we have shown that particularly for markers of fibrosis (Figure 3B), regardless of the microbiome
26 status, the mice developed significant injury. For CD8+ T cells, F4/80+ macrophages and overall CD45+
27 leukocytes, we observed significant changes in GF and COL mice, although GF mice tended to show a
28 higher fold change in response to HTN (Supplemental Table 2). Despite these similarities, both cardiac
29 hypertrophy (Figure 2A) and left ventricular mass-to-tibia length (Figure 2B) were significantly altered
30 upon HTN induction in the GF but not COL mice. Nonetheless, our data suggest that the kidney, more so
31 than the heart, represents a subspace of hypertensive target organ damage, which is more susceptible to
32 microbial colonization. It is conceivable that cardiac damage could be further exacerbated as renal
33 function declines. Thus, the gut microbiota could be added as an important modulator of the well-known
34 cardio-renal axis. Further research to follow up this idea is required, perhaps using several iterations of
35 variations to a defined community of microbes, to test the universality of this hypothesis.

36 Metabolites of microbial origin, some of which are known to be associated with cardiovascular disease
37 and accumulate in chronic kidney disease^{16, 17}, were measurable within the serum metabolome of our

1 COL but not our GF mice, such as IS and TMAO (Supplemental Figure S1D). Our results very clearly
2 indicate that GF mice experience robust kidney damage to a greater extent than COL mice, despite GF
3 mice being devoid of these harmful metabolites. However, we suggest that the reason COL mice
4 experience less overall damage is likely due to the presence of SCFA. We and others have shown the
5 potent effect of SCFA in mouse models.^{13, 14} Here we have shown again, for a representative set of
6 animals, that SCFA are depleted in GF mice (Figure 5C). We hypothesize that the potency of SCFA in
7 COL mice counterbalances the presence of IS and TMAO. Further research on this topic is required to
8 definitively conclude the effects of the co-occurrence of these various metabolites of microbial origin.
9 Furthermore, we show that systemic inflammatory response to HTN is altered by colonization status.
10 MSDC, which represent an important subset of innate anti-inflammatory cells in HTN⁹, reacted differently
11 GF mice compared to COL (Figure 6C-D). Additionally, we found that Th17 cells were increased during
12 HTN in GF mice (Figure 6E). Th1-like Th17 cells, which are known to be pathogenic, trended towards
13 enrichment in GF+HTN mice (Figure 6F). We wanted to explore *in vitro* that naïve T cells from GF mice
14 were more sensitive to polarizing cytokines and Ang II. We found that upon polarization, naïve T cells
15 from GF mice skewed more towards Th17, particularly when Ang II was added (Figure 6G). As it has
16 been recently demonstrated that the SCFA propionate can decrease the rate of Th17 cell differentiation^{41,}
17 ⁴², we suspected that this could be part of the reason naïve cells from COL mice were less inducible
18 toward Th17. Indeed, when we pre-treated naïve CD4+ T cells with butyrate and propionate, we observed
19 a decline in Th17 inducibility in the presence of Ang II in GF; an effect that was not seen in cells isolated
20 from CONV mice (Figure 6H). Recently, Krebs and colleagues showed that the development of Th17 cells
21 in the kidney is dependent on the cytokine micromilieu and can be blocked with specific antibodies
22 against IL-1b and IL-6.⁴⁵ We also could show that the polarization conditions used in our Th17 *in vitro*
23 assay were practically available *in vivo*, and the expression of each polarizing cytokine was increased
24 within heart and kidney tissue of hypertensive mice.

25 To our knowledge, one study similar to ours exists within the literature, published by Karbach et al.⁴⁶ It is
26 clear from the extensive phenotyping performed in our study that our findings were not congruent with
27 their data, where they showed that GF mice were protected from developing HTN and related vascular
28 damage. Though this was initially a surprise, upon further examination, there are two likely scenarios that
29 may explain this. First, the protocol of our experiments did differ from one another. The study from
30 Karbach and colleagues compared GF mice to conventionally raised mice, whereas we compared GF
31 mice with littermates that had been colonized early in life. Therefore, our study was able to account for
32 known genetic drifts in gnotobiotic colonies. Additionally, Ang II infusion was only performed for seven
33 days, while we studied a more chronic phenotype. Furthermore, our mice ate different diets, and as Kaye
34 and colleagues recently demonstrated, the composition of the diet can have a profound impact on the
35 resultant hypertensive phenotype.⁴⁷ Second, it is highly likely that the microbiome used in our study and
36 in the study by Karbach and colleagues may be distinct from one another. Incongruencies like ours have
37 also been found in other contexts. The comparison of microbiome-rich and GF mice in one study showed

1 the amelioration of an IRI of the kidney by the microbiome⁴³, where another study demonstrated the
2 opposite effect⁴⁸.

3 To investigate the second scenario further, we hypothesized that the microbiome background used in any
4 given study might have drastic implications for the study outcome. Our group and others have shown that
5 microbially-produced metabolites have a potent effect on the pathogenesis of HTN.^{5, 13, 14, 49} In reference
6 to that, if the microbiota itself were to change, we expect the circulating metabolites to be likewise altered
7 within the host. Unfortunately, the study from Karbach et al.⁴⁶ did not include any information regarding
8 the microbiome and metabolome of their microbiota-rich mice. Although, we did find a recent study from
9 Cheema and Pluznick²⁰ where these data were made available, but their phenotypic data is not
10 reported.²⁰ Nevertheless, to test our hypothesis regarding the putative comparability of the colonizing
11 microbiome between studies, and the impact this may have on resultant study outcome, we decided to
12 compare our microbiome and metabolome to the published data from Cheema and Pluznick. To compare
13 the microbiomes from these two studies, we re-annotated our shotgun microbiome sequencing data such
14 that it would be comparable to the 16s rDNA sequencing data from Cheema and Pluznick. The
15 microbiome of colonized mice between the two studies were starkly contrasting in sham and HTN mice
16 (shown as a multivariate PCoA plot derived from genus level information from each of the studies,
17 Supplemental Figure S10A). We surmised that because of the lack of overlapping microbiome signatures
18 within our study and the Pluznick dataset, that the metabolome signal would likewise be dichotomous. We
19 compared the serum metabolome dataset from the two studies by using metabolites which could be
20 measured in both studies from all COL and GF mice. We found that interestingly, there was significantly
21 less distance between the effect of HTN on individual metabolites within the serum metabolome of GF
22 mice from these two studies than in the equivalent COL mice comparison (Supplemental Figure S10B-C).
23 This result suggests that the congruence of the serum metabolome in GF groups within these two
24 datasets is higher than the COL groups. These exploratory data support the idea that the structure of the
25 implanted microbiome has a measurable impact on serum metabolome alterations in response to HTN.
26 Because of our and others' findings regarding the importance of microbial metabolites in HTN, we believe
27 that this could be a driving factor behind the contradictory phenotypic results of our study compared to the
28 data from Karbach et al.⁴⁶. It is nonetheless critical in future studies for the microbiome to be well
29 documented and openly accessible to avoid questions regarding the reproducibility of existing studies.

30

31 **Conclusion**

32 We have shown that the microbiota has a profound effect on hypertensive disease pathogenesis.
33 Furthermore, we have shown that GF mice, when compared to their colonized littermates, experienced an
34 aggravation of target organ damage, which was more distinct in the kidney than in the heart. Additionally,
35 we demonstrated that the metabolome is influenced significantly by the microbiome used for
36 experimentation, which underscores the need for standardization of experimentation and reporting within
37 the field. The immunophenotype of HTN mice, and in particular, the alteration of MDSC and Th17 cells,

1 which have been previously implicated in HTN, give us some indication of how GF mice may have
2 developed an exacerbated hypertensive phenotype in our study. *In vitro*, SCFA rescued the pro-
3 inflammatory phenotype of T cells isolated from GF mice. We propose that the COL mice were protected
4 from damage in comparison to their GF counterparts due to the absence of the potent anti-inflammatory
5 SCFA metabolites under GF conditions.

7 **Author Contributions**

8 N.W., D.N.M., H.B. designed the study. E.G.A., H.B., A.R., G.N., D.T., A.Y., C.Z., L. Y., L.M., A.M.,
9 A.P. and N.W. performed animal experiments and analyzed the data. A.F.R, M.T., and M.B. performed *in*
10 *vivo* BP measurement. T.U.P.B. and U.L. performed the microbiome analysis. E.G.A., R.F.G., S.K. and
11 J.A.K performed and analyzed the metabolomics experiments. S.K.F. and C.Y.C. helped with data
12 analysis and interpretation. E.G.A., N.W., H.B., and D.N.M. wrote the manuscript with input from all
13 authors.

15 **Funding**

16 N.W. is supported by the European Research Council (ERC) under the European Union's Horizon 2020
17 research and innovation program (852796) and by a grant from the Corona-Stiftung im Deutschen
18 Stiftungszentrum, Essen, Germany. A.P., N.W., D.N.M., and S.K.F. are supported by the Deutsche
19 Forschungsgemeinschaft (DFG, German Research Foundation) Projektnummer 394046635 - SFB 1365.
20 The DZHK (German Centre for Cardiovascular Research, 81Z1100101) supported D.N.M. N.W. was
21 participant in the Clinician Scientist Program funded by the Berlin Institute of Health (BIH).

23 **Acknowledgments**

24 We thank Petra Voss, Ilona Kramer, May-Britt Köhler, Jana Czychi, Ute Gerhardt, Alina Eisenberger,
25 Martin Taube, and Stefanie Schelenz for their technical assistance.

27 **Disclosures**

28 None.

30 **Data availability statement**

31 The data underlying this article are available in the article and in its online supplementary material. The
32 microbiome data underlying this article are available in NCBI database and can be accessed as
33 BioProject PRJNA812410. The metabolomics data underlying this article are available via FigShare,
34 please see supplementary table 10 for access links.

1 **References**

- 2 1. Ezzati M, Riboli E. Behavioral and dietary risk factors for noncommunicable diseases. *N Engl J*
3 *Med* 2013;**369**:954-964.
- 4 2. Avery EG, Bartolomaeus H, Maifeld A, Marko L, Wiig H, Wilck N, Rosshart SP, Forslund SK, Muller
5 DN. The Gut Microbiome in Hypertension: Recent Advances and Future Perspectives. *Circulation*
6 *research* 2021;**128**:934-950.
- 7 3. Madhur MS, Elijovich F, Alexander MR, Pitzer A, Ishimwe J, Van Beusecum JP, Patrick DM, Smart
8 CD, Kleyman TR, Kingery J, Peck RN, Laffer CL, Kirabo A. Hypertension: Do Inflammation and
9 Immunity Hold the Key to Solving this Epidemic? *Circ Res* 2021;**128**:908-933.
- 10 4. Verhaar BJH, Collard D, Prodan A, Levels JHM, Zwinderman AH, Backhed F, Vogt L, Peters MJL,
11 Muller M, Nieuwdorp M, van den Born BH. Associations between gut microbiota, faecal short-
12 chain fatty acids, and blood pressure across ethnic groups: the HELIUS study. *Eur Heart J*
13 2020;**41**:4259-4267.
- 14 5. Wilck N, Matus MG, Kearney SM, Olesen SW, Forslund K, Bartolomaeus H, Haase S, Mahler A,
15 Balogh A, Marko L, Vvedenskaya O, Kleiner FH, Tsvetkov D, Klug L, Costea PI, Sunagawa S, Maier
16 L, Rakova N, Schatz V, Neubert P, Fratzer C, Krannich A, Gollasch M, Grohme DA, Corte-Real BF,
17 Gerlach RG, Basic M, Typas A, Wu C, Titze JM, Jantsch J, Boschmann M, Dechend R,
18 Kleinewietfeld M, Kempa S, Bork P, Linker RA, Alm EJ, Muller DN. Salt-responsive gut commensal
19 modulates TH17 axis and disease. *Nature* 2017;**551**:585-589.
- 20 6. Yang T, Santisteban MM, Rodriguez V, Li E, Ahmari N, Carvajal JM, Zadeh M, Gong M, Qi Y,
21 Zubcevic J, Sahay B, Pepine CJ, Raizada MK, Mohamadzadeh M. Gut dysbiosis is linked to
22 hypertension. *Hypertension* 2015;**65**:1331-1340.
- 23 7. Madhur MS, Lob HE, McCann LA, Iwakura Y, Blinder Y, Guzik TJ, Harrison DG. Interleukin 17
24 promotes angiotensin II-induced hypertension and vascular dysfunction. *Hypertension*
25 2010;**55**:500-507.
- 26 8. Marko L, Kvakan H, Park JK, Qadri F, Spallek B, Binger KJ, Bowman EP, Kleinewietfeld M, Fokuhl
27 V, Dechend R, Muller DN. Interferon-gamma signaling inhibition ameliorates angiotensin II-
28 induced cardiac damage. *Hypertension* 2012;**60**:1430-1436.
- 29 9. Shah KH, Shi P, Giani JF, Janjulia T, Bernstein EA, Li Y, Zhao T, Harrison DG, Bernstein KE, Shen XZ.
30 Myeloid Suppressor Cells Accumulate and Regulate Blood Pressure in Hypertension. *Circulation*
31 *research* 2015;**117**:858-869.

- 1 10. Ivanov, II, Atarashi K, Manel N, Brodie EL, Shima T, Karaoz U, Wei D, Goldfarb KC, Santee CA,
2 Lynch SV, Tanoue T, Imaoka A, Itoh K, Takeda K, Umesaki Y, Honda K, Littman DR. Induction of
3 intestinal Th17 cells by segmented filamentous bacteria. *Cell* 2009;**139**:485-498.
- 4 11. Zaccane P, Raine T, Sidobre S, Kronenberg M, Mastroeni P, Cooke A. Salmonella typhimurium
5 infection halts development of type 1 diabetes in NOD mice. *Eur J Immunol* 2004;**34**:3246-3256.
- 6 12. Tan J, McKenzie C, Potamitis M, Thorburn AN, Mackay CR, Macia L. The role of short-chain fatty
7 acids in health and disease. *Adv Immunol* 2014;**121**:91-119.
- 8 13. Marques FZ, Nelson E, Chu PY, Horlock D, Fiedler A, Ziemann M, Tan JK, Kuruppu S, Rajapakse
9 NW, El-Osta A, Mackay CR, Kaye DM. High-Fiber Diet and Acetate Supplementation Change the
10 Gut Microbiota and Prevent the Development of Hypertension and Heart Failure in Hypertensive
11 Mice. *Circulation* 2017;**135**:964-977.
- 12 14. Bartolomaeus H, Balogh A, Yakoub M, Homann S, Marko L, Hoges S, Tsvetkov D, Krannich A,
13 Wundersitz S, Avery EG, Haase N, Kraker K, Hering L, Maase M, Kusche-Vihrog K, Grandoch M,
14 Fielitz J, Kempa S, Gollasch M, Zhumadilov Z, Kozhakhmetov S, Kushugulova A, Eckardt KU,
15 Dechend R, Rump LC, Forslund SK, Muller DN, Stegbauer J, Wilck N. Short-Chain Fatty Acid
16 Propionate Protects From Hypertensive Cardiovascular Damage. *Circulation* 2019;**139**:1407-
17 1421.
- 18 15. Poll BG, Cheema MU, Pluznick JL. Gut Microbial Metabolites and Blood Pressure Regulation:
19 Focus on SCFAs and TMAO. *Physiology (Bethesda)* 2020;**35**:275-284.
- 20 16. Zhu W, Gregory JC, Org E, Buffa JA, Gupta N, Wang Z, Li L, Fu X, Wu Y, Mehrabian M, Sartor RB,
21 McIntyre TM, Silverstein RL, Tang WHW, DiDonato JA, Brown JM, Luscis AJ, Hazen SL. Gut
22 Microbial Metabolite TMAO Enhances Platelet Hyperreactivity and Thrombosis Risk. *Cell*
23 2016;**165**:111-124.
- 24 17. Nakano T, Katsuki S, Chen M, Decano JL, Halu A, Lee LH, Pestana DVS, Kum AST, Kuromoto RK,
25 Golden WS, Boff MS, Guimaraes GC, Higashi H, Kauffman KJ, Maejima T, Suzuki T, Iwata H,
26 Barabasi AL, Aster JC, Anderson DG, Sharma A, Singh SA, Aikawa E, Aikawa M. Uremic Toxin
27 Indoxyl Sulfate Promotes Proinflammatory Macrophage Activation Via the Interplay of OATP2B1
28 and Dll4-Notch Signaling. *Circulation* 2019;**139**:78-96.
- 29 18. Marko L, Park JK, Henke N, Rong S, Balogh A, Klamer S, Bartolomaeus H, Wilck N, Ruland J,
30 Forslund SK, Luft FC, Dechend R, Muller DN. B-cell lymphoma/leukaemia 10 and angiotensin II-
31 induced kidney injury. *Cardiovasc Res* 2020;**116**:1059-1070.

- 1 19. Leelahavanichkul A, Yan Q, Hu X, Eisner C, Huang Y, Chen R, Mizel D, Zhou H, Wright EC, Kopp JB,
2 Schnermann J, Yuen PS, Star RA. Angiotensin II overcomes strain-dependent resistance of rapid
3 CKD progression in a new remnant kidney mouse model. *Kidney Int* 2010;**78**:1136-1153.
- 4 20. Cheema MU, Pluznick JL. Gut Microbiota Plays a Central Role to Modulate the Plasma and Fecal
5 Metabolomes in Response to Angiotensin II. *Hypertension* 2019;**74**:184-193.
- 6 21. Mishima E, Ichijo M, Kawabe T, Kikuchi K, Akiyama Y, Toyohara T, Suzuki T, Suzuki C, Asao A, Ishii
7 N, Fukuda S, Abe T. Germ-Free Conditions Modulate Host Purine Metabolism, Exacerbating
8 Adenine-Induced Kidney Damage. *Toxins (Basel)* 2020;**12**.
- 9 22. Richards DA, Aronovitz MJ, Calamaras TD, Tam K, Martin GL, Liu P, Bowditch HK, Zhang P,
10 Huggins GS, Blanton RM. Distinct Phenotypes Induced by Three Degrees of Transverse Aortic
11 Constriction in Mice. *Sci Rep* 2019;**9**:5844.
- 12 23. Joe B, McCarthy CG, Edwards JM, Cheng X, Chakraborty S, Yang T, Golonka RM, Mell B, Yeo JY,
13 Bearss NR, Furtado J, Saha P, Yeoh BS, Vijay-Kumar M, Wenceslau CF. Microbiota Introduced to
14 Germ-Free Rats Restores Vascular Contractility and Blood Pressure. *Hypertension* 2020;**76**:1847-
15 1855.
- 16 24. Edwards JM, Roy S, Tomcho JC, Schreckenberger ZJ, Chakraborty S, Bearss NR, Saha P, McCarthy
17 CG, Vijay-Kumar M, Joe B, Wenceslau CF. Microbiota are critical for vascular physiology: Germ-
18 free status weakens contractility and induces sex-specific vascular remodeling in mice. *Vascul*
19 *Pharmacol* 2020;**125-126**:106633.
- 20 25. Mattson DL. Comparison of arterial blood pressure in different strains of mice. *Am J Hypertens*
21 2001;**14**:405-408.
- 22 26. Hoverstad T, Midtvedt T. Short-chain fatty acids in germfree mice and rats. *J Nutr*
23 1986;**116**:1772-1776.
- 24 27. Smith K, McCoy KD, Macpherson AJ. Use of axenic animals in studying the adaptation of
25 mammals to their commensal intestinal microbiota. *Semin Immunol* 2007;**19**:59-69.
- 26 28. Kamali AN, Noorbakhsh SM, Hamedifar H, Jadidi-Niaragh F, Yazdani R, Bautista JM, Azizi G. A
27 role for Th1-like Th17 cells in the pathogenesis of inflammatory and autoimmune disorders. *Mol*
28 *Immunol* 2019;**105**:107-115.
- 29 29. Coit P, Dozmorov MG, Merrill JT, McCune WJ, Maksimowicz-McKinnon K, Wren JD, Sawalha AH.
30 Epigenetic Reprogramming in Naive CD4+ T Cells Favoring T Cell Activation and Non-Th1 Effector

- 1 T Cell Immune Response as an Early Event in Lupus Flares. *Arthritis Rheumatol* 2016;**68**:2200-
2 2209.
- 3 30. Altorok N, Coit P, Hughes T, Koelsch KA, Stone DU, Rasmussen A, Radfar L, Scofield RH, Sivils KL,
4 Farris AD, Sawalha AH. Genome-wide DNA methylation patterns in naive CD4+ T cells from
5 patients with primary Sjogren's syndrome. *Arthritis Rheumatol* 2014;**66**:731-739.
- 6 31. Heninger AK, Eugster A, Kuehn D, Buettner F, Kuhn M, Lindner A, Dietz S, Jergens S, Wilhelm C,
7 Beyerlein A, Ziegler AG, Bonifacio E. A divergent population of autoantigen-responsive CD4(+) T
8 cells in infants prior to beta cell autoimmunity. *Sci Transl Med* 2017;**9**.
- 9 32. Li J, Zhao F, Wang Y, Chen J, Tao J, Tian G, Wu S, Liu W, Cui Q, Geng B, Zhang W, Weldon R,
10 Auguste K, Yang L, Liu X, Chen L, Yang X, Zhu B, Cai J. Gut microbiota dysbiosis contributes to the
11 development of hypertension. *Microbiome* 2017;**5**:14.
- 12 33. Adnan S, Nelson JW, Ajami NJ, Venna VR, Petrosino JF, Bryan RM, Jr., Durgan DJ. Alterations in
13 the gut microbiota can elicit hypertension in rats. *Physiol Genomics* 2017;**49**:96-104.
- 14 34. Santisteban MM, Qi Y, Zubcevic J, Kim S, Yang T, Shenoy V, Cole-Jeffrey CT, Lobaton GO, Stewart
15 DC, Rubiano A, Simmons CS, Garcia-Pereira F, Johnson RD, Pepine CJ, Raizada MK. Hypertension-
16 Linked Pathophysiological Alterations in the Gut. *Circ Res* 2017;**120**:312-323.
- 17 35. Kashyap S, Osman M, Ferguson CM, Nath MC, Roy B, Lien KR, Nath KA, Garovic VD, Lerman LO,
18 Grande JP. Ccl2 deficiency protects against chronic renal injury in murine renovascular
19 hypertension. *Sci Rep* 2018;**8**:8598.
- 20 36. Eardley KS, Zehnder D, Quinkler M, Lepenies J, Bates RL, Savage CO, Howie AJ, Adu D, Cockwell
21 P. The relationship between albuminuria, MCP-1/CCL2, and interstitial macrophages in chronic
22 kidney disease. *Kidney Int* 2006;**69**:1189-1197.
- 23 37. Pindjakova J, Hanley SA, Duffy MM, Sutton CE, Weidhofer GA, Miller MN, Nath KA, Mills KH,
24 Ceredig R, Griffin MD. Interleukin-1 accounts for intrarenal Th17 cell activation during ureteral
25 obstruction. *Kidney Int* 2012;**81**:379-390.
- 26 38. Andrade-Oliveira V, Amano MT, Correa-Costa M, Castoldi A, Felizardo RJ, de Almeida DC, Bassi
27 EJ, Moraes-Vieira PM, Hiyane MI, Rodas AC, Peron JP, Aguiar CF, Reis MA, Ribeiro WR, Valduga
28 CJ, Curi R, Vinolo MA, Ferreira CM, Camara NO. Gut Bacteria Products Prevent AKI Induced by
29 Ischemia-Reperfusion. *J Am Soc Nephrol* 2015;**26**:1877-1888.
- 30 39. Singh N, Thangaraju M, Prasad PD, Martin PM, Lambert NA, Boettger T, Offermanns S,
31 Ganapathy V. Blockade of dendritic cell development by bacterial fermentation products

- 1 butyrate and propionate through a transporter (Slc5a8)-dependent inhibition of histone
2 deacetylases. *The Journal of biological chemistry* 2010;**285**:27601-27608.
- 3 40. Wang F, Liu J, Weng T, Shen K, Chen Z, Yu Y, Huang Q, Wang G, Liu Z, Jin S. The Inflammation
4 Induced by Lipopolysaccharide can be Mitigated by Short-chain Fatty Acid, Butyrate, through
5 Upregulation of IL-10 in Septic Shock. *Scand J Immunol* 2017;**85**:258-263.
- 6 41. Duscha A, Gisevius B, Hirschberg S, Yissachar N, Stangl GI, Eilers E, Bader V, Haase S, Kaisler J,
7 David C, Schneider R, Troisi R, Zent D, Hegelmaier T, Dokalis N, Gerstein S, Del Mare-Roumani S,
8 Amidror S, Staszewski O, Poschmann G, Stuhler K, Hirche F, Balogh A, Kempa S, Trager P, Zaiss
9 MM, Holm JB, Massa MG, Nielsen HB, Faissner A, Lukas C, Gatermann SG, Scholz M, Przuntek H,
10 Prinz M, Forslund SK, Winklhofer KF, Muller DN, Linker RA, Gold R, Haghikia A. Propionic Acid
11 Shapes the Multiple Sclerosis Disease Course by an Immunomodulatory Mechanism. *Cell*
12 2020;**180**:1067-1080 e1016.
- 13 42. Haghikia A, Jorg S, Duscha A, Berg J, Manzel A, Waschbisch A, Hammer A, Lee DH, May C, Wilck
14 N, Balogh A, Ostermann AI, Schebb NH, Akkad DA, Grohme DA, Kleinewietfeld M, Kempa S,
15 Thone J, Demir S, Muller DN, Gold R, Linker RA. Dietary Fatty Acids Directly Impact Central
16 Nervous System Autoimmunity via the Small Intestine. *Immunity* 2015;**43**:817-829.
- 17 43. Jang HR, Gandolfo MT, Ko GJ, Satpute S, Racusen L, Rabb H. Early exposure to germs modifies
18 kidney damage and inflammation after experimental ischemia-reperfusion injury. *Am J Physiol*
19 *Renal Physiol* 2009;**297**:F1457-1465.
- 20 44. Mishima E, Fukuda S, Mukawa C, Yuri A, Kanemitsu Y, Matsumoto Y, Akiyama Y, Fukuda NN,
21 Tsukamoto H, Asaji K, Shima H, Kikuchi K, Suzuki C, Suzuki T, Tomioka Y, Soga T, Ito S, Abe T.
22 Evaluation of the impact of gut microbiota on uremic solute accumulation by a CE-TOFMS-based
23 metabolomics approach. *Kidney Int* 2017;**92**:634-645.
- 24 45. Krebs CF, Reimers D, Zhao Y, Paust HJ, Bartsch P, Nunez S, Roseblatt MV, Hellmig M, Kilian C,
25 Borchers A, Enk LUB, Zinke M, Becker M, Schmid J, Klinge S, Wong MN, Puelles VG, Schmidt C,
26 Bertram T, Stumpf N, Hoxha E, Meyer-Schwesinger C, Lindenmeyer MT, Cohen CD, Rink M, Kurts
27 C, Franzenburg S, Koch-Nolte F, Turner JE, Riedel JH, Huber S, Gagliani N, Huber TB, Wiech T,
28 Rohde H, Bono MR, Bonn S, Panzer U, Mittrucker HW. Pathogen-induced tissue-resident
29 memory TH17 (TRM17) cells amplify autoimmune kidney disease. *Sci Immunol* 2020;**5**.
- 30 46. Karbach SH, Schonfelder T, Brandao I, Wilms E, Hormann N, Jackel S, Schuler R, Finger S, Knorr
31 M, Lagrange J, Brandt M, Waisman A, Kossmann S, Schafer K, Munzel T, Reinhardt C, Wenzel P.

- 1 Gut Microbiota Promote Angiotensin II-Induced Arterial Hypertension and Vascular Dysfunction.
2 *J Am Heart Assoc* 2016;**5**.
- 3 47. Kaye DM, Shihata WA, Jama HA, Tsyganov K, Ziemann M, Kiriazis H, Horlock D, Vijay A, Giam B,
4 Vinh A, Johnson C, Fiedler A, Donner D, Snelson M, Coughlan MT, Phillips S, Du XJ, El-Osta A,
5 Drummond G, Lambert GW, Spector TD, Valdes AM, Mackay CR, Marques FZ. Deficiency of
6 Prebiotic Fiber and Insufficient Signaling Through Gut Metabolite-Sensing Receptors Leads to
7 Cardiovascular Disease. *Circulation* 2020;**141**:1393-1403.
- 8 48. Emal D, Rampanelli E, Stroo I, Butter LM, Teske GJ, Claessen N, Stokman G, Florquin S, Leemans
9 JC, Dessing MC. Depletion of Gut Microbiota Protects against Renal Ischemia-Reperfusion Injury.
10 *J Am Soc Nephrol* 2017;**28**:1450-1461.
- 11 49. Heianza Y, Ma W, Manson JE, Rexrode KM, Qi L. Gut Microbiota Metabolites and Risk of Major
12 Adverse Cardiovascular Disease Events and Death: A Systematic Review and Meta-Analysis of
13 Prospective Studies. *J Am Heart Assoc* 2017;**6**.

14

1 **Figure Legends**

2 **Figure 1. Renal damage is exacerbated under germ-free conditions.** A) Description of experimental
 3 protocol (unless otherwise stated, GF Sham n = 5, GF + HTN n = 12, COL Sham n = 5, COL + HTN
 4 n = 12 for further analyses). B) Urinary albumin-to-creatinine ratio from spot urine collected upon sacrifice
 5 from a subset of mice (COL n = 5, COL + HTN n = 5, GF n = 4, GF + HTN n = 6). C) *Lcn2* gene
 6 expression was measured from kidney tissue by qPCR. D) Histological kidney sections were stained for
 7 nephrin. Representative glomeruli are shown (left). Nephrin immunofluorescence was quantified as mean
 8 fluorescence intensity (MFI) in the glomerular space averaged per mouse. The scale bar represents 20
 9 μm . E) Macrophages (F4/80+), (F) CD8+, and (G) CD4+ T cells from kidney sections were counted from
 10 5 representative high-power fields within the cortex. For (B-G), the left graph was tested using a two-way
 11 ANOVA and post-hoc Sidak multiple comparison's test and depicts the raw values for each variable. For
 12 (B-F), hypertension was identified as the source of variation using two-way ANOVA, and post-hoc multiple
 13 comparison between sham and HTN within each group revealed that the GF comparison was the source
 14 of variation. In (G), hypertension was identified as the source of variation using two-way ANOVA, and
 15 post-hoc multiple comparison between sham and HTN within each group revealed that both the GF and
 16 COL comparison were significant. For B through G, the right plot depicts the relative change induced by
 17 Ang II + 1% NaCl in comparison to the respective sham group, tested using an unpaired two-tailed T-test.
 18 No change (100%) depicted as dotted line. For all plots, p-values are as follows; * $P \leq 0.05$, ** $P \leq 0.01$,
 19 *** $P \leq 0.001$, **** $P \leq 0.0001$.

20
 21 **Figure 2. Cardiac inflammation and hypertrophy are aggravated in GF mice.** Unless otherwise
 22 stated, GF Sham n = 5, GF + HTN n = 12, COL Sham n = 5, COL + HTN n = 12. A) Heart weight to tibia
 23 length [g/m] from mice taken at sacrifice. B) Left ventricular (LV) mass was estimated using
 24 echocardiography and normalized to tibia length [g/m]. C) Cardiac ventricular natriuretic peptide gene
 25 expression (*Nppb*) measured by qPCR. COL + HTN n = 11, otherwise as stated above. D)
 26 Echocardiography prior to sacrifice revealed no change in the ejection fraction upon HTN induction in GF
 27 or COL mice. E) Perivascular fibrosis from cardiac vessels, evaluated by measuring the fibrotic area
 28 relative to the medial area of vessels from Collagen 1 stained histology slides. GF Sham n=4, otherwise
 29 as stated above.. F) Cardiac interstitial fibrosis was evaluated as fibronectin positive area proportionate to
 30 total area from 5 representative 40x magnification pictures from histological slides. In scale bar
 31 represents 40 μm . G) Macrophages (F4/80+) were counted from 5 representative high-power fields, and
 32 (H) CD4+, and (I) CD8+ T cells were counted from whole heart sections. Two-way ANOVA and post-hoc
 33 Sidak multiple comparison's test for (A-I) was used to test significance in the left plot. In (A-C) and (E-F),
 34 hypertension was identified as the source of variation using two-way ANOVA, and post-hoc multiple
 35 comparison between sham and HTN within each group revealed that the GF comparison was the source
 36 of variation. In (G) hypertension and the microbiome were both identified as sources of variation using
 37 two-way ANOVA, and significant post-hoc comparisons are shown. In (I), hypertension was identified as

1 the source of variation using two-way ANOVA, and post-hoc multiple comparison between sham and
 2 HTN within each group revealed that both the GF and COL comparison were significant. To the right in
 3 (A-I), the relative change induced by Ang II + 1% NaCl in comparison to the respective sham group was
 4 tested using an unpaired two-tailed T-test. No change (100%) depicted as dotted line. For all plots, p-
 5 values are as follows; * $P \leq 0.05$, ** $P \leq 0.01$, *** $P \leq 0.001$.

6
 7 **Figure 3. Unbiased assessment of kidney and heart damage in HTN treated GF vs COL mice.**

8 Unless otherwise stated, GF Sham $n = 5$, GF + HTN $n = 12$, COL Sham $n = 5$, COL + HTN $n = 12$. For
 9 cardiac RNA expression COL + HTN $n = 11$, otherwise as stated before. A) Effect sizes (Cliff's delta [D])
 10 and fold changes are shown to assess the effect of HTN treatment relative to the respective sham group
 11 in GF and COL on the kidney phenotype. Color and triangle direction indicates effect size. Size indicates
 12 \log_2 -transformed fold change (Log2FC) of HTN compared to the respective sham group. Significance
 13 was calculated using the Mann-Whitney U-test and was FDR-corrected with the Benjamini-Hochberg
 14 procedure to account for multiple testing. Markers for significant Q-values are superimposed, and
 15 transparency indicates non-significant effects. $^{\circ}q < 0.1$, $^*q < 0.05$, $^{**}q < 0.01$. Variables are organized by
 16 subcategory (Damage, Fibrosis, Inflammation). B) Same univariate analysis as in A) was performed on
 17 cardiac phenotypic data. Variables are organized by subcategory (Function, Hypertrophy, Fibrosis,
 18 Inflammation). C) Principal Coordinate analysis was performed based on Euclidean distance scaling of
 19 kidney phenotypic data to demonstrate the dissimilarities between study groups in a quantitative
 20 phenotypic state space. Pairwise comparisons between groups were performed using PERMANOVA and
 21 reported in the inset table. D) Principal Coordinate analysis as in C) was performed on the cardiac
 22 phenotypic data.

23
 24 **Figure 4. Blood pressure and Angiotensin II reactivity in GF and COL mice.** $N = 5$ animals per group.

25 A) GF and COL mice were implanted an arterial catheter for blood pressure measurement. Mean arterial
 26 pressure was measured in resting and awake animals, and the difference was tested using an unpaired
 27 two-tailed t-test (** $P \leq 0.01$). B) The increase in blood pressure after acute intravenous infusion of
 28 Angiotensin II as a bolus was measured. No statistical difference between GF and COL mice was found
 29 using a two-way repeated measurement ANOVA ($p = 0.14$), whereas Ang II dose had a significant
 30 influence ($p \leq 0.0001$, not shown).

31
 32 **Figure 5. Microbiome heavily influences the metabolome in response to HTN.** Unless otherwise

33 stated, GF Sham $n = 5$, GF + HTN $n = 12$, COL Sham $n = 5$, COL + HTN $n = 12$. A) Using the Biocrates
 34 MxP500 Quant kit, serum metabolites were analyzed from GF and COL mice. Metabolites were grouped
 35 by class to demonstrate the overall effect on the serum metabolome. Effect size (Cliff's delta [D]) is shown
 36 to demonstrate the effect of HTN relative to the respective sham group in GF and COL. Colour and
 37 triangle direction indicates effect size. Size indicates \log_2 -transformed fold change (Log2FC) of HTN mice

1 compared to the respective sham group. Significance was calculated using the Mann-Whitney U test and
 2 was FDR-corrected using the Benjamini-Hochberg procedure to account for multiple testing. Markers for
 3 significant Q-values are superimposed, and transparency indicates non-significant effects. $^{\circ}q < 0.1$,
 4 $*q < 0.05$, $**q < 0.01$. For (B) and (C), individual metabolites rather than metabolite classes within the GF
 5 and COL group were compared using the effect size calculation listed in (A, Supplemental Table 11).
 6 Those metabolites which were significantly altered in the sham to HTN comparison, as tested using the
 7 Mann-Whitney U test with Benjamini-Hochberg FDR correction were selected and separated based on
 8 the directionality of their shift. Metabolites which decreased (B) or increased (C) in HTN relative to sham
 9 are compared between the COL and GF conditions using a Venn diagram. The number of metabolites
 10 and the percentage within each subcategory are overlaid. In (D) significant changes to individual
 11 metabolites (points) are shown in GF (y-axis) and COL (x-axis) as log₂ fold changes in response to HTN.
 12 Metabolites exclusively significantly regulated in GF or in COL are shown in red and blue, respectively.
 13 Purple points indicate metabolites significantly regulated similarly in GF and COL (significant in both and
 14 same trajectory), while black points indicate metabolites regulated significant in both groups but with
 15 opposite trajectories. Grey points are metabolites which were reliably measured but not significantly
 16 altered in either group. E) Fecal short-chain fatty acids (SCFA) from GF or CONV mice demonstrates the
 17 absence of potent anti-hypertensive metabolites butyrate and propionate in the GF setting (GF n=6,
 18 CONV n=4). Significance was tested using unpaired two-tailed Student's t-test ($***p \leq 0.001$, $****p \leq$
 19 0.0001). LC-MS, liquid chromatography-mass spectrometry; FIA-MS, flow injection analysis-mass
 20 spectrometry.

21
 22 **Figure 6. Colonization status influences the inflammatory reaction to HTN.** Unless otherwise stated,
 23 GF Sham n = 5, GF + HTN n = 12, COL Sham n = 5, COL + HTN n = 12. A) Several unique immune cell
 24 subsets were measured from the spleen, as a proxy measure of systemic inflammation. Effect size (Cliff's
 25 delta [D]) is shown to demonstrate the effect of HTN relative to the respective sham group in GF and
 26 COL. Color and triangle direction indicates effect size. Size indicates log₂-transformed fold change
 27 (Log₂FC) of HTN induction compared to the respective sham group. Significance was calculated using
 28 the Mann-Whitney U test and was FDR-corrected using the Benjamini-Hochberg procedure to account for
 29 multiple testing. Markers for significant Q-values are superimposed, and transparency indicates non-
 30 significant effects. $^{\circ}q < 0.1$, $*q < 0.05$, $**q < 0.01$. Immune cell subsets are organized by subcategory (Innate
 31 immunity and T cell overview, differentiation, and subtypes) and subsets, and cell types where no
 32 significant effect in either GF or COL was found are not shown. B) Principal Coordinate analysis was
 33 performed based on Euclidean distance scaling of immune cell abundances to demonstrate the
 34 dissimilarities between study groups. Pairwise comparisons between groups were performed using
 35 PERMANOVA and reported in the inset table. Monocytic MDSCs (mMDSC, C) and granulocytic MDSCs
 36 (gMDSC, D), as well as Th17 (E) and Th1-like Th17 cells (F) from the spleen are shown as boxplots on
 37 the left. G) Naïve CD4+ T cells from mesenteric lymph nodes of either GF or CONV mice, polarized *in*

1 *in vitro* towards a Th17 using a cocktail of IL-1 β , TGF β , and IL-6 with or without Ang II (GF n= 4, CONV n=
2 5). In (H) naïve CD4+ T cells were pre-treated with 1 mM SCFA mix (0.5 mM of each butyrate and
3 propionate) or 1 mM NaCl. Subsequently, the pre-treatment was removed, and cells were polarized
4 toward Th17 in the presence of Ang II as described in G (GF n= 6, CONV n= 6). To the left in (C-G), two-
5 way ANOVA and post-hoc Sidak multiple comparison's test was used to test significance. To the right in
6 (C-F), the relative change induced by Ang II + 1% NaCl in comparison to the respective sham group was
7 tested using an unpaired two-tailed T-test. No change (100%) depicted as dotted line. In H) for the
8 Th17+AngII and Th17+AngII+SCFA mix a one-tailed T-test was performed per group, as a pre-specified
9 hypothesis from Figure 6G was tested. For all plots in (C-G), p-values are as follows; * P \leq 0.05, ** P \leq
10 0.01.

11

12

ACCEPTED MANUSCRIPT

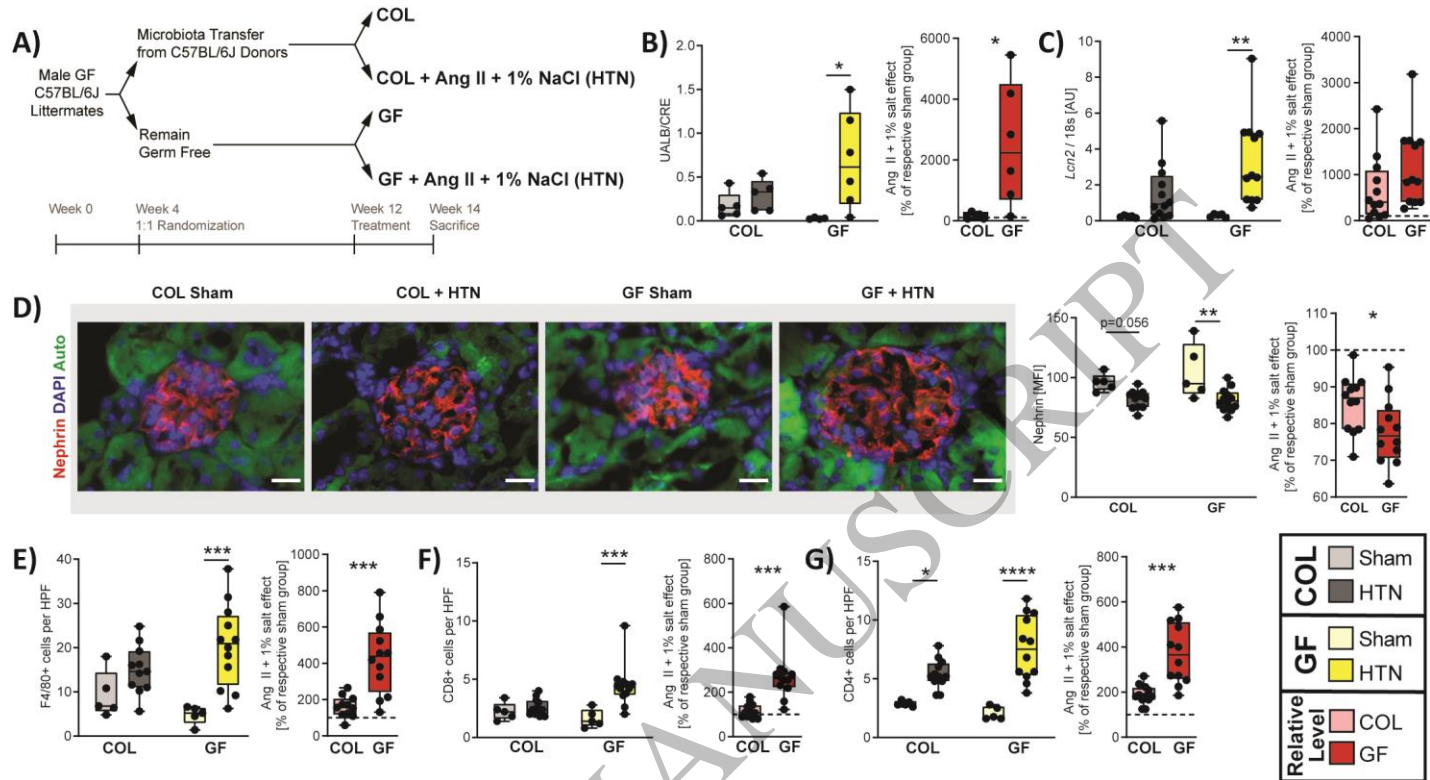


Figure 1

188x103 mm (.15 x DPI)

1
2
3
4

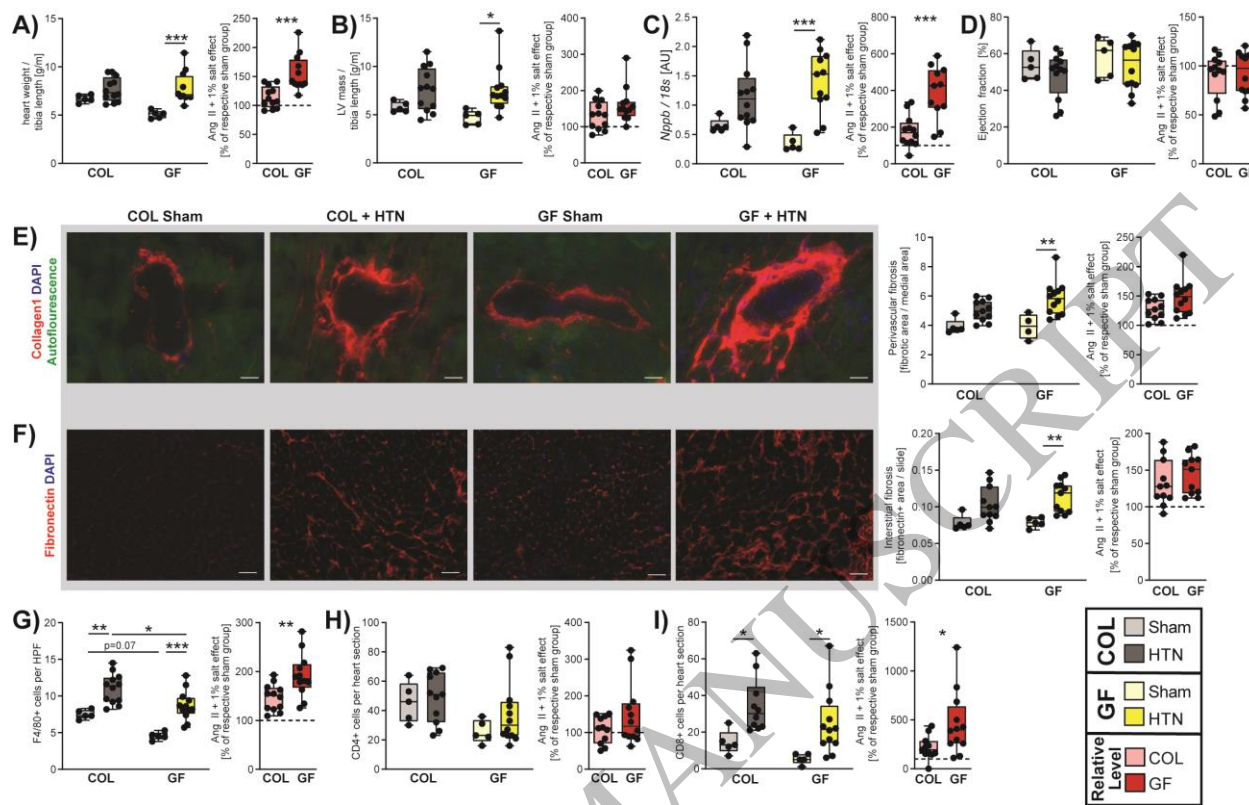
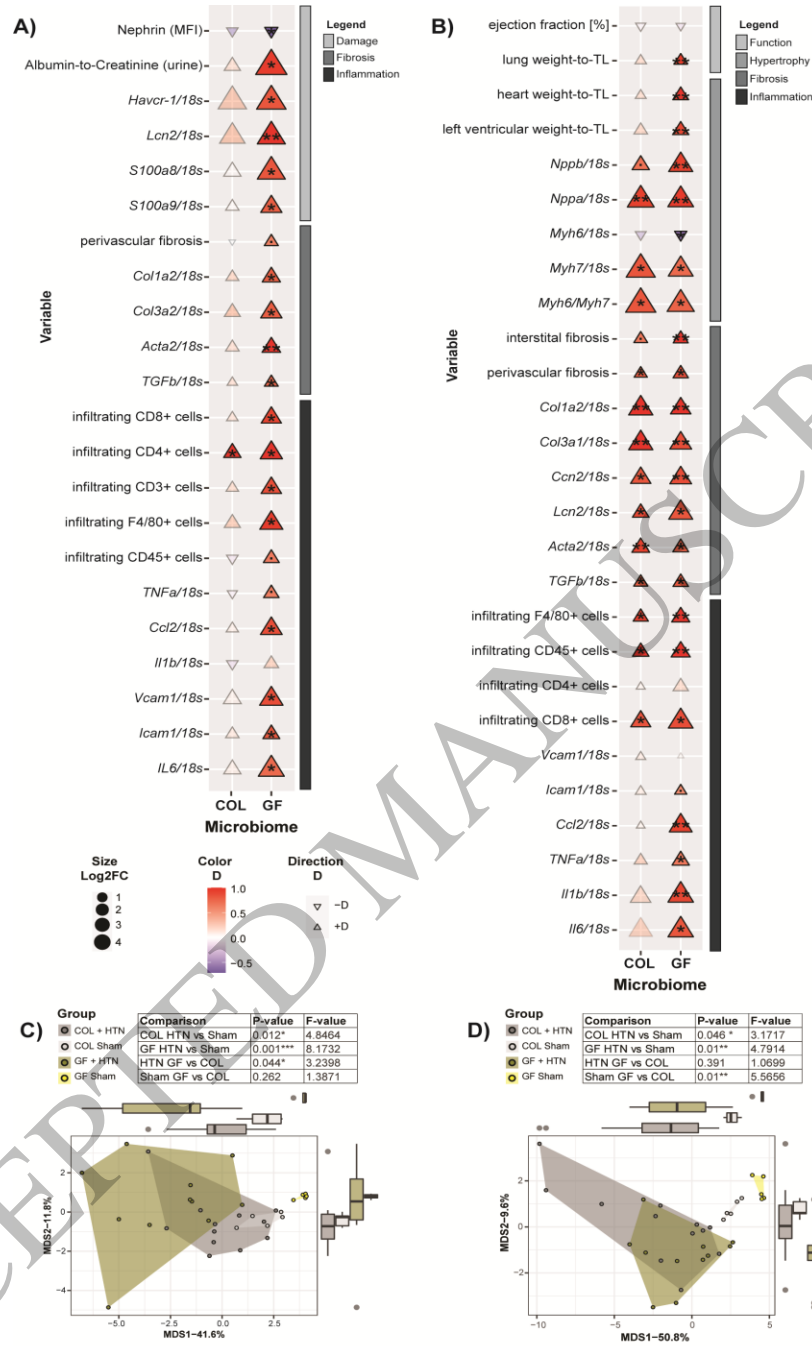


Figure 2

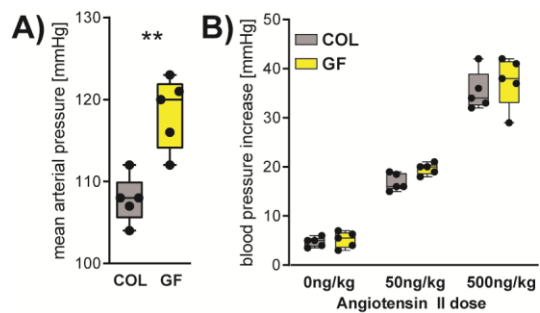
207x132 mm (.15 x DPI)

1
2
3
4



1
2
3
4

Figure 3
159x311 mm (.15 x DPI)

**Figure 4**

70x40 mm (.15 x DPI)

1
2
3
4

ACCEPTED MANUSCRIPT

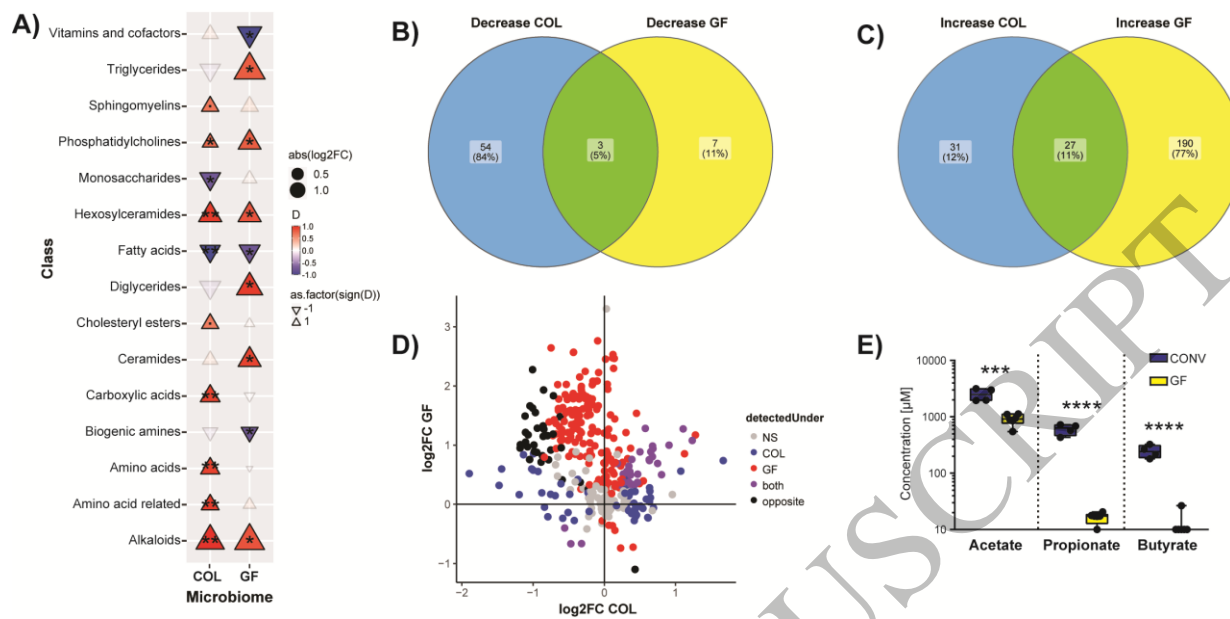


Figure 5
 198x96 mm (.15 x DPI)

1
 2
 3
 4

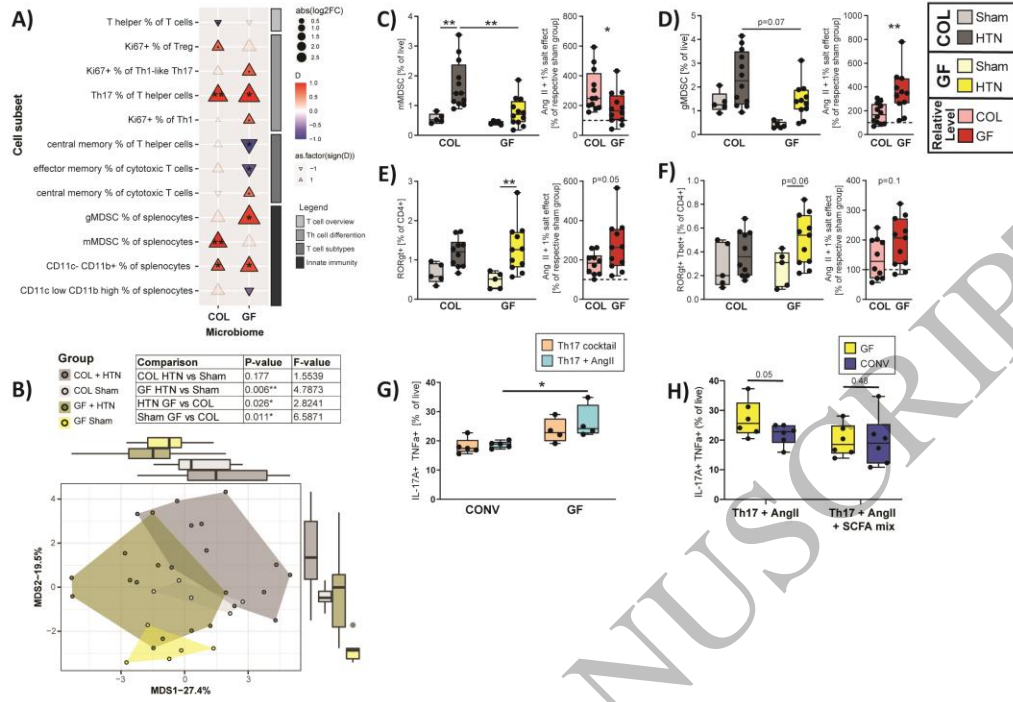


Figure 6

Figure 6
210x297 mm (.15 x DPI)

1
2
3